tan β determination from heavy Higgs boson production at linear colliders

V. Barger,* T. Han,† and J. Jiang‡
Department of Physics, University of Wisconsin, 1150 University Avenue, Madison, Wisconsin 53706
(Received 26 June 2000; published 27 February 2001)

We study the production at future e^+e^- linear colliders of the heavy neutral Higgs bosons H and A of the minimal supersymmetric standard model in association with top and bottom quarks. The cross sections have a strong dependence on the parameter tan β, and thus provide a good way to determine it. At a linear collider with $\sqrt{s}=0.5$–1 TeV and expected integrated luminosities, we find significant sensitivities for determining tan β. In the supergravity scenario, the sensitivity is particularly strong for tan $\beta \gtrsim 10$, reaching a 15% or better measurement. In the general MSSM scenario, the interplay between the $4b$ and $4t$ channels results in a good determination for tan $\beta \lesssim 10$, while the sensitivity is weakened for higher values of tan β.

DOI: 10.1103/PhysRevD.63.075002 PACS number(s): 14.80.Cp, 11.30.Pb

I. INTRODUCTION

One of the most promising avenues for physics beyond the standard model (SM) is supersymmetry (SUSY) [1], since it can provide a fundamental understanding of electroweak symmetry breaking (EWSB) and it allows unification of the electroweak and strong interactions at a grand unified scale [2]. Because of its great theoretical attraction, extensive phenomenological work continues to explore the ways for discovery and precision study of supersymmetric particles at present and future colliders.

Most of these investigations are directed to the minimal supersymmetric standard model (MSSM), which has the minimal new particle content [1]. The MSSM contains two Higgs doublets which develop vacuum expectation values $<H_1>=v_1/\sqrt{2}$ and $<H_2>=v_2/\sqrt{2}$ that break the SU(2) $\times$U(1) gauge symmetry spontaneously [3]. There are 5 physical Higgs bosons in the MSSM: two CP-even states h and H, a CP-odd state A, and two charged states $H^{\pm}$; the lightest Higgs boson is h.

The ratio $v_2/v_1=\tan\beta$ is a critical parameter of the MSSM: It characterizes the relative fraction that the two Higgs doublets contribute to the EWSB, and it enters all sectors of the theory. The interactions of both the SUSY particles and the Higgs bosons depend on tan β, and the relations of SUSY particle masses to the soft symmetry breaking parameters of supersymmetry involve tan β [3]. A measurement of tan β from one sector will thereby allow predictions or tests in other sectors. The renormalization group evolution of the Yukawa couplings from the unification scale to the electroweak scale are sensitive to the value of tan β. The large top quark mass can naturally be explained with m_b-m_τ unification as a quasi-infrared fixed point of the top Yukawa coupling if tan $\beta \simeq 1.8$ or tan $\beta \simeq 56$ [4]. The possibility of SO(10) Yukawa unification requires the high tan β solution [5]. The predicted mass of the lightest SUSY Higgs boson also depends on tan β, with $m_h \sim 105$ GeV at tan $\beta \simeq 1.8$ and $m_h \sim 120$ GeV at tan $\beta \gtrsim 20$ [6].

Because of the significance of tan β for the theory and phenomenology of the MSSM, it is important to find processes in which tan β can be best determined. Some regions of the MSSM parameter space have been excluded at LEP2 [7] due to the lower bound on the lightest Higgs boson mass (m_h), particularly at low tan β near 1. Much of the parameter space remains to be explored at the upgraded Tevatron [8,9], the LHC [10–12], the future linear colliders [13–18] and muon colliders [19]. The tan β constraints that may be obtained from m_h via radiative corrections [6], or from precision electroweak measurements [20], or from SUSY particle production usually depend also on other SUSY parameters. Furthermore, measurements of sin β or cos β via other SUSY processes without directly involving Higgs bosons do not accurately determine large tan β values [17]. For general SUSY Higgs phenomenology, we refer the readers to reviews [21].

The Higgs couplings of $H,A,H^{\pm}$ to heavy quarks are given by

$$A\bar{t}t: \frac{-gm_t}{2m_W}\cot\beta\gamma_5 \quad A\bar{b}b: \frac{-gm_b}{2m_W}\tan\beta\gamma_5 \tag{1}$$

$$H\bar{t}t: \frac{-igm_t}{2m_W}\frac{\sin\alpha}{\sin\beta} \approx \frac{igm_t}{2m_W}\cot\beta$$

$$H\bar{b}b: \frac{-igm_b}{2m_W}\frac{\cos\alpha}{\cos\beta} \approx \frac{-igm_b}{2m_W}\tan\beta \tag{2}$$

$$H^+\bar{t}b: \frac{igV_{td}}{2\sqrt{2}m_W}[(m_b\tan\beta+m_t\cot\beta) + (m_b\tan\beta-m_t\cot\beta)\gamma_5], \tag{3}$$

where the decoupling limit $M_A \gg M_Z$ has been assumed for the approximate forms of $H\bar{t}t, H\bar{b}b$. In this limit, the lightest Higgs boson h becomes SM-like and its couplings are insensitive to SUSY parameters. For the $H,A,H^{\pm}$ Higgs bosons, tan β is essentially the unique parameter for Higgs-heavy quark couplings. This suggests that studies of the associated

*Email address: barger@oriole.physics.wisc.edu
†Email address: than@egret.physics.wisc.edu
‡Email address: jiang@pheno.physics.wisc.edu

 ©2001 The American Physical Society

production of the Higgs bosons and heavy quarks may effectively probe the $\tan\beta$ parameter.

Heavy Higgs boson production at future e^+e^- colliders was discussed in Ref. [15]. In a recent study Feng and Moroi [16] evaluated the prospects for determining $\tan\beta$ in e^+e^- collisions with $\sqrt{s}=0.5$ and 1 TeV c.m. energy via the processes

$$e^+e^- \to Zh, AH, t\bar{b}H^- \quad \text{and} \quad \bar{t}bH^+. \tag{4}$$

The primary channel in their study involves the $H^+\bar{t}b$ coupling. They found that the strong dependence of heavy Higgs branching fractions on $\tan\beta$ allows stringent constraints to be placed for moderate $\tan\beta$ [16] in the MSSM. In the present paper, we report results of a complementary study of the associated production of a neutral Higgs boson and heavy quarks

$$e^+e^- \to H\bar{t}t, H\bar{b}b, A\bar{t}t, \quad \text{and} \quad A\bar{b}b. \tag{5}$$

These processes involve $\bar{t}t$ and $\bar{b}b$ production separately and are thereby expected to be complementary for low and high values of $\tan\beta$. We study the sensitivity to probe $\tan\beta$ in two scenarios: the minimal supergravity model (M SUGRA) and the MSSM.

The paper is organized as follows: We present the Higgs decay branching fractions and the cross sections for the associated production of the Higgs bosons and heavy quarks in Sec. II. We analyze the sensitivity to determine the value of $\tan\beta$ at future linear colliders in Sec. III. We discuss our results, make some general remarks and conclude in Sec. IV.

II. NEUTRAL HIGGS PRODUCTION

A. Input parameters

In MSSM at tree level, the inpute parameters in the Higgs sector are m_A and $\tan\beta$. In a general analysis including radiative corrections the parameters required are

$$m_Q, \quad m_U, \quad m_D, \quad M_1, \quad M_2, \quad A_U, \quad A_D \quad \text{and} \quad \mu, \tag{6}$$

where m_Q is the soft SUSY breaking mass parameter of left-handed stop (where only the heavy third generation parameters are relevant), $m_U(m_D)$ the SUSY breaking mass parameter of right-handed top squark (bottom squark), M_1, M_2 the gaugino masses, $A_U(A_D)$ the top squark trilinear soft breaking term, and μ the Higgs mixing parameter. The large parameter space involved makes phenomenological studies difficult. On the other hand, once a precision measurement is made in the Higgs sector in future collider experiments, we would expect to learn more about the SUSY sector due to the radiative relations among the physical SUSY masses. Instead of exploring the large space of the MSSM soft parameters, we focus on the following two scenarios for illustration.

1. M SUGRA

Motivated by the minimal supergravity (M SUGRA) model and the requirements of radiatively generated electroweak symmetry breaking (EWSB), we relate the soft SUSY breaking parameters to the common scalar, fermion and trilinear parameters m_0, $m_{1/2}$, and A_0 at the grand unified scale. For specific choices of $\tan\beta$ the results depend on the sign of μ. The $\mu>0$ sign is less constrained by $b\to s\gamma$ decay [22] and we adopt this convention in our analysis.

TABLE I. ISAJET output parameters.

$\tan\beta$	m_A	m_H	$m_{\chi^\pm}$	m_{χ^0}	μ	m_Q	m_U	m_D	A_U	A_D
3	434	438	105	56	315	360	265	411	−330	−693
10	373	373	110	57	274	359	272	406	−370	−689
30	273	273	112	59	264	337	276	364	−354	−581

We make use of the ISAJET package [23] to determine the SUSY masses and couplings from the grand unified theory (GUT) scale input parameters. The Higgs boson mass eigenvalues are among the outputs of this program. These values agree with the corresponding results from the code of Ref. [24] to a precision $\lesssim 0.3\%$. The soft-supersymmetry-breaking parameters are evolved according to renormalization group (RG) equations [4,25,26]. For our illustrations we make the parameter choice $m_0=250$ GeV, $m_{1/2}=150$ GeV, $A_0=-300$ GeV, along with the positive sign of μ. The magnitude of μ is fixed in terms of M_Z through the radiately generated EWSB. For three representative $\tan\beta$ values, the mass eigenvalues of Higgs bosons and SUSY soft-breaking terms are listed in Table I. For charginos and neutralinos, we list only the masses of the lightest ones. In fact, our choice of the above parameters is somewhat conservative in exploring the SUSY Higgs sector. A large m_0 results in heavy $H, A, H^\pm$. Consequently it leads to the ''decoupling limit'' [27] so that the lightest Higgs boson h becomes SM-like and thus insensitive to the SUSY parameters.

2. MSSM

We also perform the same study in the MSSM scenario, in which $\tan\beta$ as well as the masses of the Higgs bosons (determined by m_A) are all free parameters to explore. The choice of other input parameters is as follows:

$$\mu=272 \text{ GeV}, \quad m_Q=356 \text{ GeV}, \quad m_U=273 \text{ GeV}, \tag{7}$$

$$m_D=400 \text{ GeV}, \quad A_U=-369 \text{ GeV}, \quad A_D=-672 \text{ GeV} \tag{8}$$

$$m_{\chi^\pm}=111 \text{ GeV}, \quad m_{\chi^0}=59 \text{ GeV}. \tag{9}$$

These soft SUSY breaking parameters are similar to M SUGRA parameters with $\tan\beta\approx 15$. In particular we study two cases with $m_A=200$ GeV and 400 GeV, while m_H is nearly degenerate with m_A. These choices represent the kinematical situations for A, H to be below and above $t\bar{t}$ threshold.

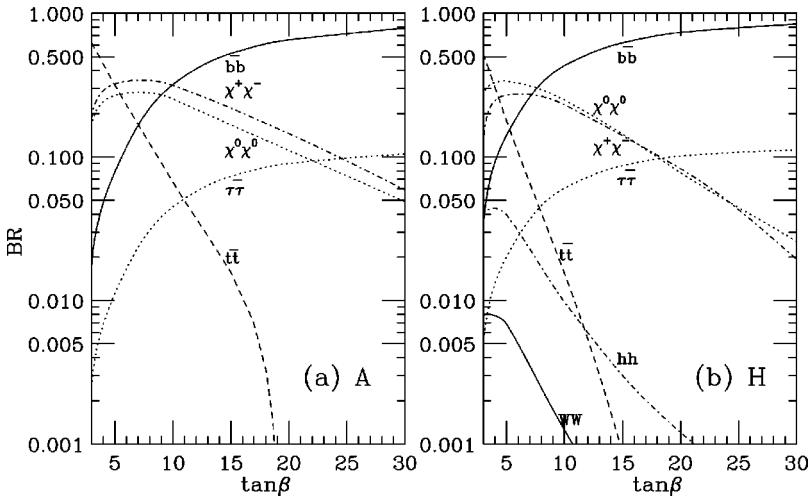

FIG. 1. M SUGRA: Leading branching fractions of decays (a) of A and (b) of H versus $\tan\beta$.

B. Branching fractions

We use the program provided in Ref. [24] for obtaining the branching fractions for the Higgs boson decay. In this program all kinematically allowed decay channels in MSSM are included and RG improved values of Higgs boson masses and couplings with the main NLO corrections [6] are implemented.

In Fig. 1 we plot the branching fraction of the decays (a) for A and (b) for H versus $\tan\beta$ in M SUGRA. As $\tan\beta$ increases, the branching fractions of A and H decay into $t\bar{t}$ drop rapidly and the decays into $b\bar{b}$ increase dramatically. The branching fractions into chargino and neutralino pairs peak at intermediate values $\tan\beta\sim 5$ and can be as large as 30%. Branching fractions of H decay into hh and WW are also shown in Fig. 1(b) for comparison. With this strong dependence of the branching fractions on $\tan\beta$, we expect neutral Higgs production channels to be useful in determining the value of $\tan\beta$. In particular, it is interesting to note the complementarity between $t\bar{t}$ and $b\bar{b}$ modes for small and large values of $\tan\beta$.

In the MSSM scenario, for the case of $m_A=200$ GeV, Fig. 2 shows the branching fraction of the decays of A and H versus $\tan\beta$. Note that the $t\bar{t}$ channel is not open. For the case of $m_A=400$ GeV, the corresponding branching fractions are shown in Fig. 3. We see that Figs. 1 and 3 are alike due to similar kinematical thresholds.

C. Cross sections and final state signature

As a representative example of the processes in Eq. (5), the tree-level Feynman diagrams for $e^+e^-\to Ht\bar{t}$ are shown in Fig. 4. For the other processes, we simply need to replace H with A, or/and $t\bar{t}$ with $b\bar{b}$. The last diagram in Fig. 4 involving the ZZH coupling is unique to the process which has H in the final state. We have included both the diagrams of Higgs radiation off a heavy quark ($Ht\bar{t}$) and Higgs decay ($HA\to Ht\bar{t}$). QCD corrections to these processes have been recently calculated [28] and found to be moderate at the energies of current interest. It is important to note that the $H(A)$ decay processes are sensitive to $\tan\beta$ only when the branching fractions vary rapidly. The $H,A\to b\bar{b}$ branching fractions gradually approach unity at large $\tan\beta$, and the dependence on $\tan\beta$ is thus reduced here. On the other hand, diagrams with $H(A)$ radiation off a heavy quark typically have a quadratic dependence on $\tan\beta$, and are thus quite sensitive to $\tan\beta$.

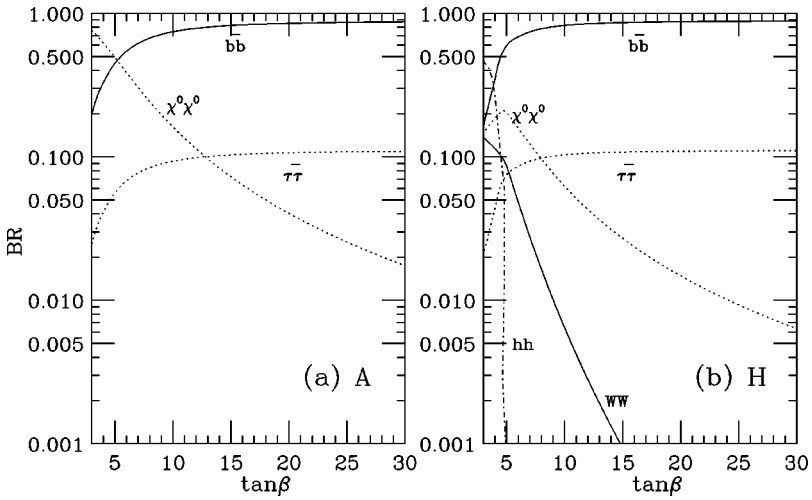

FIG. 2. MSSM: Leading branching fractions of decays with $m_A=200$ GeV (a) of A and (b) of H versus $\tan\beta$.

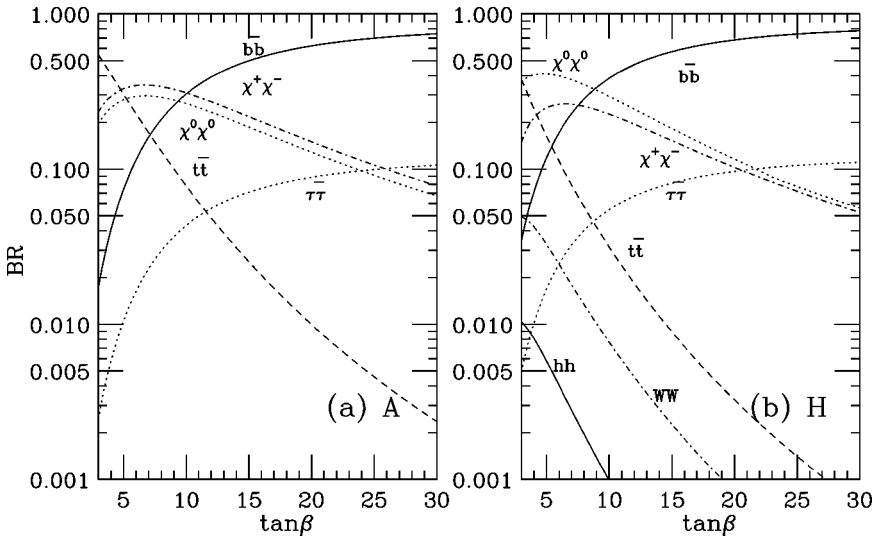

FIG. 3. MSSM: Leading branching fractions of decays with $m_A=400$ GeV (a) of A and (b) of H versus $\tan\beta$.

Figure 5 shows the calculated total cross sections of the processes $e^+e^-\to A(H)t\bar{t}, A(H)b\bar{b}$ versus the center of mass energy ($\sqrt{s}$) for $\tan\beta=3$ and 30 in the MSUGRA scenario. The cross sections for $Ab\bar{b}, At\bar{t}$ can be typically of 0.1–10 fb for this range of $\tan\beta$ at linear collider energies of 0.5–2 TeV. The maximum rate is reached at a c.m. energy about 300 GeV or so above the $At\bar{t}$ threshold. Note the different mass thresholds in this figure for the two values of $\tan\beta$, as given by the masses in Table I. For the heavy Higgs bosons under consideration, we concentrate on a collider energy $\sqrt{s}\sim 1$ TeV. We plot the cross sections versus $\tan\beta$ in Fig. 6(a) in the MSUGRA scenario. At low $\tan\beta$ the associated production of A with $t\bar{t}$ is dominant but this channel is greatly suppressed at large $\tan\beta$ values. On the other hand, the production of A in association with $b\bar{b}$ is small at low $\tan\beta$ and increases rapidly with $\tan\beta$. Figure 6(b) shows the cross sections similar to Fig. 6(a) but in the MSSM scenario for cases: $m_A=200$ GeV at $\sqrt{s}=500$ GeV (solid) and 400 GeV at $\sqrt{s}=1$ TeV (dashes). The associated production of H with $t\bar{t}$ or $b\bar{b}$ has similar characteristics to A production.

Concerning the final state signature with the $A(H)$ decays, we notice that at low $\tan\beta$, both the production cross section for $At\bar{t}$ ($Ht\bar{t}$) and the branching fraction for $A(H)$ decay into $t\bar{t}$ are large as a result of the typical $(\cot\beta)^4$ enhancement. The $e^+e^-\to t\bar{t}t\bar{t}$ signal is dominant at low $\tan\beta$ but at high $\tan\beta$, $e^+e^-\to b\bar{b}b\bar{b}$ becomes dominant because of the $(\tan\beta)^4$ enhancement. For intermediate values of $\tan\beta\sim 5$, the SUSY decay modes, such as $A,H\to\chi^+\chi^-$ and $\chi^0\chi^0$ can be more important. We show in Fig. 7(a) the total cross sections at $\sqrt{s}=1$ TeV versus $\tan\beta$ including the different final states. The complementarity of the three final states in different range of $\tan\beta$ can be seen in this figure. Figure 7(b) again shows the contribution of these final states for $\tan\beta$ values where they are most important: $4b$ for $\tan\beta=30$, $b\bar{b}\chi^{\mp}\chi^{\mp}$, or $b\bar{b}\chi^0\chi^0$ for $\tan\beta=10$, and $4t$ for $\tan\beta=3$. The $4b$ standard model background is also shown by the dot-dashed curve.

In the MSSM scenario, similar curves for the $4t$ and $4b$ final state signals are shown in Fig. 8 for two cases: $m_A=200$ GeV at $\sqrt{s}=0.5$ TeV and $m_A=400$ GeV at $\sqrt{s}=1$ TeV.

D. Background

The most robust channels, $b\bar{b}b\bar{b}$ and $t\bar{t}t\bar{t}$, from neutral Higgs production have rather small SM backgrounds. The SM expectation for $e^+e^-\to b\bar{b}b\bar{b}$ production is shown in Fig. 7(b). The cross section decreases with increasing $\sqrt{s}$ as $(1/\sqrt{s})^2$. At $\sqrt{s}=1$ TeV, the $4b$ background is only 0.1 fb, much smaller than the signal rate at large $\tan\beta$. The SM cross section for $e^+e^-\to t\bar{t}t\bar{t}$ is smaller than 10^{-3} fb at

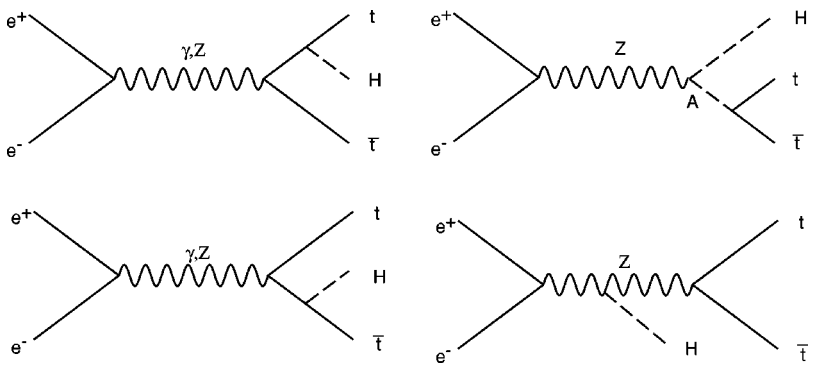

FIG. 4. Feynman diagrams contributing to $e^+e^-\to Ht\bar{t}$. The diagrams for $e^+e^-\to At\bar{t}$ are similar, except that the last diagram above is absent.

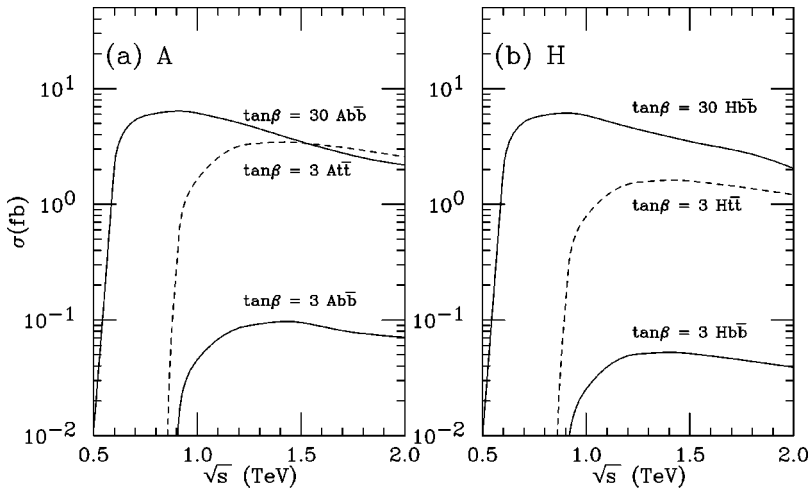

FIG. 5. M SUGRA: Total Higgs production cross sections versus the center of mass energy with $\tan\beta=3$ and 30 (a) for $e^+e^-\to At\bar{t}$ (dashes) and $Ab\bar{b}$ (solid) and (b) for $e^+e^-\to Ht\bar{t}$ (dashes) and $Hb\bar{b}$ (solid).

$\sqrt{s}=1$ TeV and thus is negligible. The SM $4b$ background at 500 GeV is about 3.7 fb. We take this background into consideration when we calculate the limits at $\sqrt{s}=500$ GeV. Since the SM backgrounds are small relative to the signals of interest, we do not need to impose sophisticated kinematical cuts and the signal rates are thereby better preserved. The final states involving the gauginos may have rather large SM backgrounds from $b\bar{b}$,$t\bar{t}$, gauge boson production. We neglect those channels in our evaluation.

III. ANALYSES AND RESULTS

As the parameter $\tan\beta$ is varied from small to intermediate to large values, the dominant Higgs signal comes from the three channels $t\bar{t}t\bar{t}$, $b\bar{b}\chi\chi$, $b\bar{b}b\bar{b}$, respectively. Since the sizes of the signal cross sections depend sensitively on $\tan\beta$, a determination of $\tan\beta$ should be possible throughout $\tan\beta$ ranges where there are substantial signal event rates. In our analyses, we employ the $t\bar{t}t\bar{t}$ signal at low $\tan\beta$ and the $b\bar{b}b\bar{b}$ signal at large $\tan\beta$. For the intermediate $\tan\beta$ values, we combine these two channels. We do not include the channels with gaugino final state in our consideration since the signatures would depend upon other SUSY parameters such as the slepton and squark masses. We thus regard the results of our analyses to be conservative.

We consider a $\sqrt{s}=1$ TeV collider with three integrated luminosities of 50, 100 and 500 fb^{-1}. After applying the geometrical cut

$$\cos(\theta_b)<0.9 \tag{10}$$

to the $4b$ signals, the total cross section is reduced to 23%, which we take as the geometrical efficiency. Because of the low background cross section, we only need low purity of b-tagging; we assume a b-tagging efficiency, $\epsilon_b\approx 65\%$ [29]. Since b-quark flavors are conserved in the production process, we can relax the requirement to tag only three b-quarks, as is a standard practice. Then the efficiency of detecting $3b$ in a $4b$ sample is $4\epsilon_b^3-3\epsilon_b^4\approx 56\%$. For the $4t$ channel, although the event kinematics would be more involved, the distinctive event topology compared to the SM multi-jet backgrounds should allow a clear signal separation. Nonetheless, we still require the identification of at least three b quarks. At a given $\tan\beta$ value, we multiply the total cross section of $4t$ or $4b$ channel with the geometrical efficiency, the b-tagging efficiency, and the integrated luminosity to get the signal event rate N_S. The statistical standard deviation is $\sigma=\sqrt{N_S}$. In the presence of SM backgrounds, we similarly

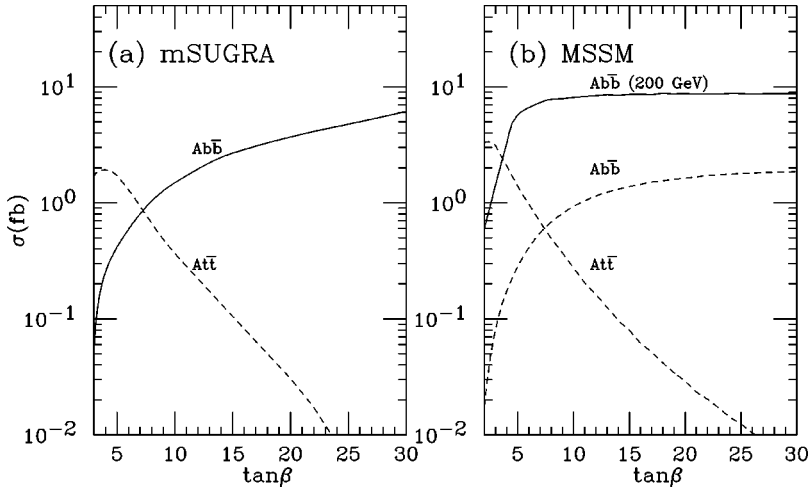

FIG. 6. Total Higgs production cross sections for $e^+e^-\to At\bar{t}$ and $Ab\bar{b}$ versus $\tan\beta$ (a) in M SUGRA at $\sqrt{s}=1$ TeV and (b) in MSSM for $m_A=200$ GeV at $\sqrt{s}=500$ GeV (solid) and for $m_A=400$ GeV at $\sqrt{s}=1$ TeV (dashes).

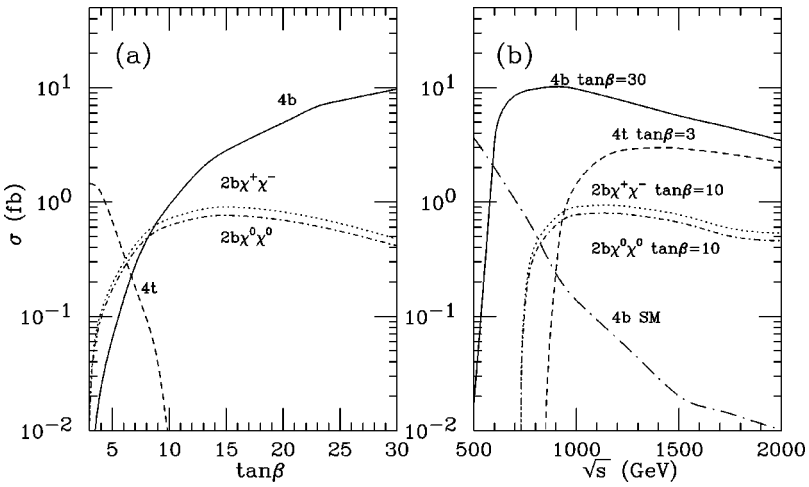

FIG. 7. M SUGRA: Total cross sections with different final states including A,H decays (a) versus $\tan\beta$ at $\sqrt{s}=1$ TeV, and (b) versus $\sqrt{s}$ for representative values of $\tan\beta=3$, 10, and 30. The SM expectation of $4b$ production is also included for comparison.

determine the background event rate N_B. We then take the conservative estimate for the signal fluctuation

$$\sigma=\sqrt{N_S+N_B}. \tag{11}$$

For a 95% confidence level (C.L.) cross section measurement, the range for the number of events is taken to be $N_S \pm 1.96\sigma$. The corresponding bounds on the signal cross sections can be translated into allowed ranges $\Delta\tan\beta$ given by

$$\Delta\tan\beta=\tan\beta_{\pm}-\tan\beta, \tag{12}$$

where $\tan\beta$ is determined from N_S and $\tan\beta_{\pm}$ is determined from $N_S\pm 1.96\sqrt{N_S+N_B}$.

We first consider the M SUGRA scenario at a $\sqrt{s}=1$ TeV linear collider. We combine both A and H channels. In Fig. 9, the 95% C.L. constraints on $\Delta\tan\beta$ for 50 fb^{-1} (solid), 100 fb^{-1} (dashes) and 500 fb^{-1} (dotted) are shown versus $\tan\beta$. We find encouraging results for the $\tan\beta$ determination. For instance, with a luminosity of 100 fb^{-1}, $|\Delta\tan\beta|\approx 3$ or better can be reached at the low value of $\tan\beta$, mainly via the $4t$ channel. At the high value of $\tan\beta$, $|\Delta\tan\beta|\approx 5$ can be reached, mainly via the $4b$ channel, which is better than 15% accuracy. The slightly more difficult region is $\tan\beta\approx 6-7$, where the $4t$ and $4b$ channels both yield smaller contributions. We expect that the inclusion of the chargino channels would improve the determination. Nevertheless, a good determination has been seen for the whole $\tan\beta$ range of interest.

We next consider the MSSM Scenario. For the case with $m_A=200$ GeV, the $A,H\to t\bar{t}$ decay channel is closed and we only make use of the processes with $4b$ in the final state. With the lower Higgs boson masses, it is sufficient to consider a linear collider with $\sqrt{s}=500$ GeV. The 95% C.L. constraints on the $\tan\beta$ determination are show in Fig. 10(a) for 100 fb^{-1} (solid), 200 fb^{-1} (dashes) and 500 fb^{-1} (dotted). In Fig. 10(b) we compare our result for 100 fb^{-1} (solid) with that obtained by Feng and Moroi (dot-dashed) [16] and they are comparable. For the case with m_A

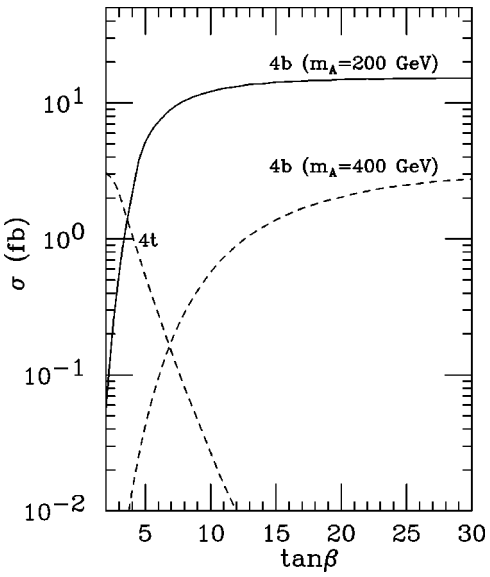

FIG. 8. MSSM: Total cross sections with $4t$ and $4b$ final states including A,H decays versus $\tan\beta$. The solid curve is for $m_A=200$ GeV at $\sqrt{s}=500$ GeV; the dashes are for $m_A=400$ GeV at $\sqrt{s}=1$ TeV.

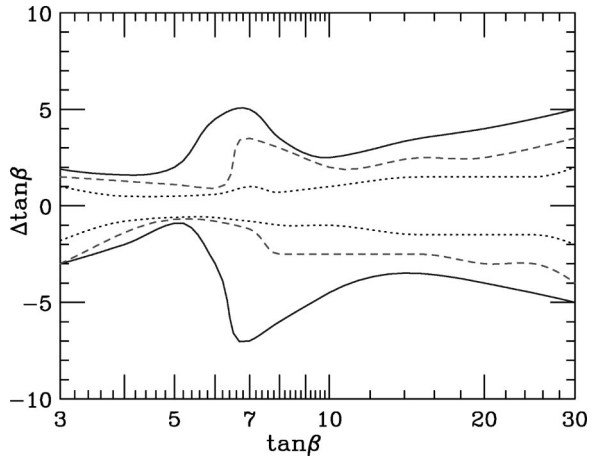

FIG. 9. M SUGRA: Determination of $\tan\beta$ at $\sqrt{s}=1$ TeV combining both A and H channels; 95% C.L. constraints on the $\tan\beta$ values are shown for 50 fb^{-1} (solid), 100 fb^{-1} (dashes) and 500 fb^{-1} (dotted).

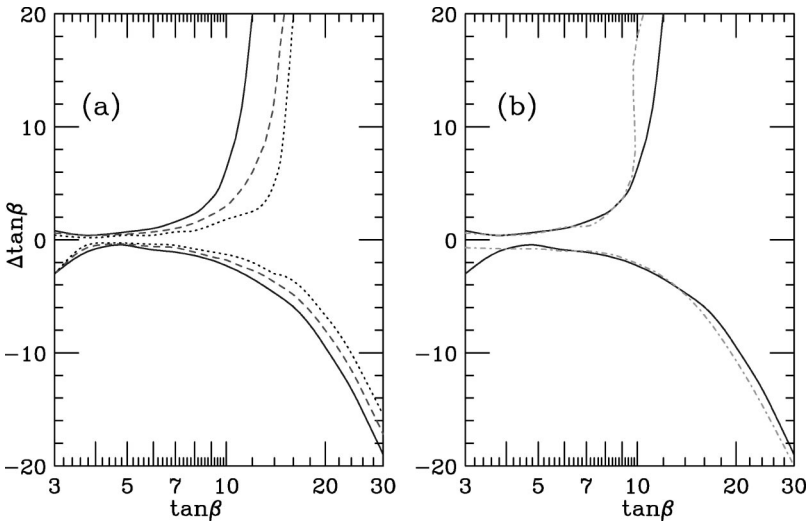

FIG. 10. MSSM: Determination of $\tan\beta$ for $m_A=200$ GeV at $\sqrt{s}=500$ GeV. (a) 95% C.L. constraints on the $\tan\beta$ values for 100 fb^{-1} (solid), 200 fb^{-1} (dashes) and 500 fb^{-1} (dotted). (b) Comparison of 95% C.L. constraints on $\tan\beta$ for 100 fb^{-1} of our result (solid) with that obtained from Ref. [16] (dot-dashed).

$=400$ GeV, the constraints on $\tan\beta$ values are shown in Fig. 11, similar to the previous figure. Since the $4t$ channel is available in this case, the determination at low $\tan\beta$ is significantly improved. For most values of $\tan\beta$, in particular higher values, we get more stringent constraints than the results in [16], indicating the potential of better determination on $\tan\beta$ via the neutral H and A channels under consideration. We list our $\tan\beta$ constraints in Table II based on a 100 fb^{-1} integrated luminosity and compare with the values that we estimate from the results by Feng and Moroi [16], where a different statistical procedure of χ^2 was adopted. The results are largely comparable, but our constraints are somewhat tighter, especially for higher values of $\tan\beta$ as already seen in Fig. 11(b).

IV. DISCUSSION AND CONCLUSION

For the M SUGRA scenario, $\tan\beta$ is essentially the only variable after fixing the other soft SUSY breaking parameters. The masses of the H,A Higgs bosons decrease as $\tan\beta$ increases. Thus the corresponding Higgs branching fractions and the production cross sections at a given energy increase with $\tan\beta$, especially for large values. This leads to possible accurate determinations of $\tan\beta$ in M SUGRA (Fig. 9), for high values in particular. In contrast, for the MSSM scenario the masses of A and H are independent of $\tan\beta$, and are kept fixed in the analyses. At large $\tan\beta$ values the decay branching fractions and the production cross sections of A or H with $b\bar{b}$ reach a plateau in the MSSM. Consequently the determination of $\tan\beta$ in that range is less effective.

There are other processes by which $\tan\beta$ may also be constrained: (i) Chargino pair production in e^+e^- collisions can provide good measurements on $\tan\beta$ for low $\tan\beta$ values [13,18]; (ii) $\tilde{\tau}_L-\tilde{\tau}_R$ mixing can be a sensitive probe of $\tan\beta$ [14]; (iii) gaugino production in $e\gamma$ collisions may provide information on $\tan\beta$ [17]; (iv) kinematical distributions from the decay products of SUSY particles can be used to determine the $\tan\beta$ value [11]; (v) the magnetic dipole moment of the muon may be useful for $\tan\beta\gtrsim 20$ if slepton masses $m_{\tilde{l}}\lesssim 300$ GeV [30]; (vi) the branching fractions of $H,A\to\tau\bar{\tau}$ may be useful to set a lower bound $\tan\beta\gtrsim 10$ [10,31]. The alternative methods in (i)–(iv) probe either $\sin\beta$ or $\cos\beta$; thus the sensitivity to $\tan\beta$ is degraded at high values of $\tan\beta$. On the other hand, methods (v) and (vi) are only effective for high values of $\tan\beta$. In contrast, Higgs

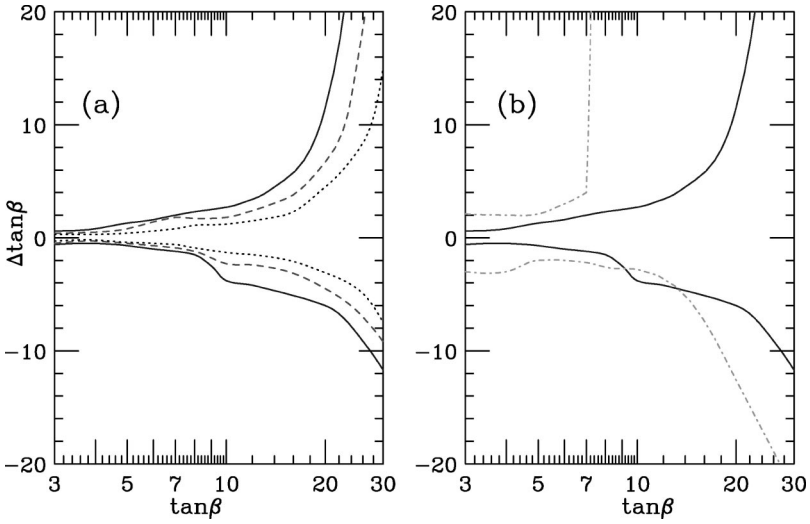

FIG. 11. MSSM: Determination of $\tan\beta$ for $m_A=400$ GeV at $\sqrt{s}=1$ TeV. (a) 95% C.L. constraints on the $\tan\beta$ values for 100 fb^{-1} (solid), 200 fb^{-1} (dashes) and 500 fb^{-1} (dotted). (b) Comparison for 95% C.L. constraints on $\tan\beta$ for 100 fb^{-1} of our result (solid) with that obtained from Ref. [16] (dot-dashed).

TABLE II. Constraints on values of $\tan\beta$ by 95% C.L. statistical measurement on the cross sections combining both A and H channels in the MSSM scenario; the results of Feng and Moroi shown here are estimated from the curves in Ref. [16] based on the $t\bar{b}H^{\pm}$ process.

$\tan\beta$	This analysis	Feng and Moroi
3	$2.4<\tan\beta<3.6$	$\tan\beta<5.2$
5	$4.3<\tan\beta<6.3$	$3.0<\tan\beta<6.0$
10	$6.2<\tan\beta<12.7$	$6.5<\tan\beta$
20	$14<\tan\beta<32$	$7.5<\tan\beta<90$
30	$18<\tan\beta<80$	$8.0<\tan\beta$

boson production processes under consideration and the $t\bar{b}H^{\pm}$ process discussed in Ref. [16] are direct probes of $\tan\beta$ with the complementary constraints from $t\bar{t}$ and $b\bar{b}$ final states at low and high values of $\tan\beta$, respectively.

In summary, we studied heavy neutral Higgs boson production in the minimal supersymmetric theories at a linear collider with $\sqrt{s}=0.5-1$ TeV with the expected integrated luminosities of 50–500 fb^{-1}. The cross sections have a strong dependence on the fundamental supersymmetry parameter $\tan\beta$, and thus provide a good way to determine it. We considered the $4b$ and $4t$ final states which are sensitive and complementary in determining $\tan\beta$. In the supergravity scenario, the sensitivity is particularly good for $\tan\beta\gtrsim 10$ in comparison with other methods, reaching a 15% or better determination in a 95% C.L. cross section measurement. In the general MSSM scenario, the interplay between the $4b$ and $4t$ channels results in a good determination for $\tan\beta \lesssim 10$ (see Table II). For higher values of $\tan\beta$ the sensitivity is weakened. The accuracy of $\tan\beta$ determination is generally sufficient to distinguish theories with a low value (~ 2) from a high value (>30) and thus to provide information on testing certain GUTs scenarios.

ACKNOWLEDGMENTS

We thank J. Feng and C. Kao for valuable discussions. This work was supported in part by a DOE Grant No. DE-FG02-95ER40896 and in part by the Wisconsin Alumni Research Foundation.

[1] For recent reviews see, e.g., H. Haber, SCIPP-92/33, hep-ph/9306207; R. Arnowitt and P. Nath, in *Perspectives on Supersymmetry*, edited by G. L. Kane (World Scientific, Singapore, 1998), p. 442; M. Drees, hep-ph/9611409; S. Martin, hep-ph/9709356; X. Tata, hep-ph/9807526.

[2] J. Ellis, S. Kelley, and D. V. Nanopoulos, Phys. Lett. B **249**, 441 (1990); J. Ellis, S. Kelley, and D. V. Nanopoulos, *ibid.* **260**, 131 (1991); U. Amaldi, W. de Boer, and H. Furstenau, *ibid.* **260**, 447 (1991); P. Langacker and M. Luo, Phys. Rev. D **44**, 817 (1991).

[3] J. Gunion, H. E. Haber, G. Kane, and S. Dawson, *The Higgs Hunter's Guide* (Addison-Wesley, Redwood City, CA, 1990).

[4] V. Barger, M. S. Berger, and P. Ohmann, Phys. Rev. D **47**, 1093 (1993); **49**, 4908 (1994); M. Carena, S. Pokorski, and C. E. M. Wagner, Nucl. Phys. **B406**, 59 (1993).

[5] B. Ananthanarayan, G. Lazarides, and Q. Shafi, Phys. Rev. D **44**, 1613 (1991); L. J. Hall, R. Rattazzi, and U. Sarid, *ibid.* **50**, 7048 (1994); L. J. Hall and S. Raby, *ibid.* **51**, 6524 (1995).

[6] H. Haber and R. Hempfling, Phys. Rev. Lett. **66**, 1815 (1991); M. Carena, P. H. Chankowski, S. Porkorski, and C. Wagner, Phys. Lett. B **411**, 205 (1998); S. Heinemeyer, W. Hollik, and G. Weiglein, Phys. Rev. D **58**, 091701 (1998); Phys. Lett. B **440**, 296 (1998); R.-J. Zhang, *ibid.* **447**, 89 (1998); J. R. Espinosa and R.-J. Zhang, hep-ph/0003246.

[7] V. Ruhlmann-Kleider, talk at XIX International Symposium on Lepton and Photon Interactions at High Energies, Stanford University, 1999; A. Quadt, talk at the XXXV Rencontres de Moriond − Electroweak and Unified theories, Les Arcs, Savoie, France, 2000.

[8] CDF Collaboration, T. Affolder *et al.*, Phys. Rev. D **62**, 012004 (2000); DØ Collaboration, B. Abbott *et al.*, Phys. Rev. Lett. **82**, 4975 (1999).

[9] M. Carena, S. Mrenna, and C. E. M. Wagner, Phys. Rev. D **60**, 075010 (1999); C. Balazs, J. L. Diaz-Cruz, H. J. He, T. Tait, and C. P. Yuan, *ibid.* **59**, 055016 (1999); see also in Physics at Run II Workshop: Higgs Boson Working Group Report, http://fnth37.fnal.gov//higgs.html.

[10] CMS Collaboration, Technical Proposal, CERN/LHCC/94−38 (1994); ATLAS Collaboration, Technical Proposal, CERN/LHCC/99-14 (1999).

[11] D. Denegri, W. Majerotto, and L. Rurua, Phys. Rev. D **60**, 035008 (1999); I. Hinchliffe and F. E. Paige, *ibid.* **61**, 095011 (2000).

[12] H. Baer, C.-H. Chen, M. Drees, F. Paige, and X. Tata, Phys. Rev. D **59**, 055014 (1999).

[13] J. L. Feng, M. E. Peskin, H. Murayama, and X. Tata, Phys. Rev. D **52**, 1418 (1995); S. Y. Choi, A. Djouadi, H. S. Song, and P. M. Zerwas, Eur. Phys. J. C **8**, 669 (1999).

[14] M. M. Nojiri, K. Fujii, and T. Tsukamoto, Phys. Rev. D **54**, 6756 (1996).

[15] A. Djouadi, J. Kalinowski, P. Ohmann, and P. M. Zerwas, Z. Phys. C **74**, 93 (1997); J. F. Gunion and J. Kelly, Phys. Rev. D **56**, 1730 (1997).

[16] J. L. Feng and T. Moroi, Phys. Rev. D **56**, 5962 (1997).

[17] V. Barger, T. Han, and J. Kelley, Phys. Lett. B **419**, 233 (1998).

[18] S. Y. Choi, A. Djouadi, H. S. Song, and P. M. Zerwas, Eur. Phys. J. C **8**, 669 (1999); V. Barger, T. Han, T. Li, and T. Plehn, Phys. Lett. B **475**, 342 (2000).

[19] V. Barger, M. S. Berger, J. F. Gunion, and T. Han, Phys. Rev. Lett. **75**, 1462 (1995); Phys. Rep. **286**, 1 (1997).

[20] Y. Yamada, K. Hagiwara, and S. Matsumoto, Suppl. Prog. Theor. Phys. **123**, 195 (1996); J. Erler and D. M. Pierce, Nucl. Phys. **B526**, 53 (1998).

[21] H. E. Haber, T. Han, F. S. Merritt, and J. Womersley, in Proceedings of the 1996 DPF/DPB Summer Study on New Direc-

tions for High Energy Physics, hep-ph/9703391; J. F. Gunion, L. Poggioli, and R. Van Kooten, *ibid.* hep-ph/9703330.

[22] P. Nath and R. Arnowitt, Phys. Lett. B **336**, 395 (1994); Phys. Rev. D **54**, 2374 (1996); V. Barger, M. S. Berger, P. Ohmann, and R. J. N. Phillips, *ibid.* **51**, 2438 (1995); H. Baer and M. Brhlik, *ibid.* **55**, 3201 (1997); H. Baer, M. Brhlik, D. Castano, and X. Tata, *ibid.* **58**, 015007 (1998); M. Ciuchini, G. Degrassi, P. Gambino, and G. F. Giudice, Nucl. Phys. **B534**, 21 (1998).

[23] F. E. Paige, S. D. Protopescu, H. Baer, and X. Tata, hep-ph/9810440.

[24] A. Djouadi, J. Kalinowski, and M. Spira, Comput. Phys. Commun. **108**, 56 (1998).

[25] K. Inoue, A. Kakuto, H. Komatsu, and H. Takeshita, Prog. Theor. Phys. **68**, 927 (1982); **71**, 413 (1984).

[26] A. H. Chamseddine, R. Arnowitt, and P. Nath, Phys. Rev. Lett. **49**, 970 (1982); L. Ibañez and G. Ross, Phys. Lett. **110B**, 215 (1982); J. Ellis, D. Nanopoulos, and K. Tamvakis, *ibid.* **121B**, 123 (1983); L. J. Hall, J. Lykken, and S. Weinberg, Phys. Rev. D **27**, 2359 (1983); L. Alvarez-Gaumé, J. Polchinski, and M. Wise, Nucl. Phys. **B121**, 495 (1983).

[27] H. E. Haber and Y. Nir, Nucl. Phys. **B335**, 363 (1990).

[28] S. Dittmaier, M. Kramer, Y. Liao, M. Spira, and P. M. Zerwas, Phys. Lett. B **478**, 247 (2000).

[29] C. Damerell and D. Jackson, in Proceedings of the 1996 DPF/DPB Summer Study on New Directions for High Energy Physics.

[30] T. Moroi, Phys. Rev. D **53**, 6565 (1996).

[31] T. Plehn, D. Rainwater, and D. Zeppenfeld, Phys. Lett. B **454**, 297 (1999).